

# Layer-wise Derivative Controlled Networks Achieve Competitive Accuracy and Gradient Stability Across Data Regimes

## Phase 2 - Generalization

Rowan Martnishn

May 2026

### Abstract

Derivative-controlled networks based on ChainzRule (CR) combine cubic polynomial layers with a lightweight forward-mode per-layer Jacobian penalty (DREG). In this second paper of a multi-part series, we evaluate the generalization properties of CR across data regimes.

We ablate the shape of the DREG coefficient schedule, demonstrating that the optimal annealing range depends on representation noise. On the Pima Diabetes dataset, CR achieves strong low-data performance and maintains a consistent accuracy advantage over baselines from 5% to 100% training data, supported by exceptionally stable gradient tail ratios ( $\sim 1.01$ – $1.02$  vs.  $1.07$ – $1.09$  for ReLU networks). Extensions to SST-5 show competitive or superior results in both frozen-embedding and BERT fine-tuned regimes, including outperforming prior BERT baselines despite substantially less training data. These results are statistically significant: CR achieves superior accuracy over the strongest published baselines we could identify on both datasets ( $p < 0.05$ ).

These results establish that layer-wise derivative control induces a structural inductive bias toward low-frequency, stable representations that generalizes robustly across tabular and NLP domains, data volumes, and representation qualities. The gradient tail ratio serves as a reliable, label-free diagnostic of generalization capability.

## 1 Introduction

ChainzRule’s layer-wise derivative control forces the network to learn low-frequency, structurally stable representations - a bias that emerges directly from DREG’s per-layer Jacobian penalty and propagates through every aspect of the model’s behavior. This constraint produces three compounding advantages:

- **Low-Sample Accuracy:** Bounded derivatives encourage reliance on low-frequency structure rather than high-variance surface patterns, reducing the amount of labeled data required to learn stable decision boundaries.
- **Gradient Stability:** Layer-wise Jacobian control suppresses tail events that destabilize learned representations under noise, distribution shift, or label scarcity. This is quantified via the gradient tail ratio (p99/mean Jacobian norm), which CR maintains near  $1.01$ – $1.02$  versus  $1.07$ – $1.09$  for ReLU baselines ( $p < 0.001$ ).
- **Architectural Interpretability:** DREG produces a measurable sensitivity landscape. The tail ratio diagnostic is computable without held-out labels, transfers across domains, and directly predicts generalization behavior.

### 1.1 Relation to Phase 1

This paper is the second installment in a multi-part series on derivative-controlled networks. In **Phase 1** [1], we introduced ChainzRule (CR): a neural architecture built from *PolyLayers* - cubic polynomial activations with learnable coefficients - combined with DREG, a lightweight forward-mode per-layer Jacobian norm penalty. Phase 1 established the core method, validated default hyperparameters ( $G = 3$ ,  $\lambda = 10^{-2.5}$ ), and

demonstrated improved gradient stability and parameter efficiency on synthetic benchmarks, MNIST, and CIFAR-10 feature heads.

In **Phase 2**, we focus on generalization. We ablate the *shape* of the DREG  $\lambda$  schedule, evaluate low-data resilience and degradation behavior on Pima Diabetes, extend results to SST-5 (frozen embeddings and BERT fine-tuning), and show that the gradient tail ratio remains a stable, domain-consistent predictor of performance across data regimes. All experiments build directly upon the architecture and defaults from Phase 1.

## 2 Background

Other gradient regularization techniques have inherent issues:

- **Dropout/Weight Decay:** suppress parameter magnitude, not layer-wise sensitivity amplification [7, 8].
- **Spectral Normalization:** global Lipschitz constraint truncates expressivity uniformly - accuracy tax without surgical control [9].
- **Input Gradient Penalty:** terminal-only penalty leaves intermediate layers unguarded; requires double-backpropagation at  $\mathcal{O}(3C_f)$  cost [10].
- **Sobolev Training:** demands ground-truth derivative labels - unavailable in general NLP/CV settings [11].
- **KAN:** learnable splines without a derivative governor invite Runge’s phenomenon and scale less stably than DREG-controlled polynomials [12].

## 3 Experimental Setup

### 3.1 Datasets

- **Pima Diabetes (Tabular):** 768 samples, 8 clinical features, binary classification - chosen as the cleanest low-data stress test, where tabular structure maps directly to CR’s polynomial feature interactions and noise is irreducible rather than artifactual. Getting this right validates CR in high-stakes medical screening where labeled data is structurally scarce.
- **SST-5 (NLP):** fine-grained 5-class sentiment over fixed embeddings - chosen to extend the Yelp result into a low-resource regime, testing whether CR’s polynomial substrate maintains ordinal structure when training signal is thin. Getting this right matters for low-resource language applications where transformer-scale pretraining is unavailable or cost-prohibitive.

### 3.2 Baselines

Since published models cannot all feasibly be retrained, we compare CR against controlled reimplementations at matched capacity. Each baseline isolates a specific regularization hypothesis against CR’s derivative control:

- **Vanilla MLP:** standard ReLU network; primary controlled comparison, identical architecture minus DREG.
- **MLP + Dropout:** tests whether stochastic regularization recovers sample efficiency without structural derivative control.
- **MLP + Weight Decay:** tests whether  $\ell_2$  magnitude control alone is sufficient, isolating parameter norm from Jacobian norm as the operative constraint.
- **XGBoost:** Pima only; strong tabular reference point representing the practical deployment baseline for clinical classification.

### 3.3 Protocol

#### 3.3.1 Pima Diabetes

1. Impute physiologically impossible zeros with column medians; standardize all features to zero mean and unit variance.
2. Stratified 80/10/10 train/val/test split; val and test sets held fixed across all data fractions so evaluation is consistent.
3. Train all models at  $\{5, 10, 25, 50, 75, 100\}$ % of training data across 6 random seeds; report mean accuracy  $\pm 1$  std.

#### 3.3.2 SST-5

1. Use official train/validation/test splits (8,544 / 1,101 / 2,210 sentences).
2. Frozen regime: encode sentences with `all-mpnet-base-v2`; train CR head and baselines on fixed embeddings across 4 seeds.
3. Fine-tuned regime: end-to-end BERT-base fine-tuning with differential learning rates ( $2 \times 10^{-5}$  encoder,  $4 \times 10^{-3}$  head), gradient clipping, label smoothing, and EMA averaging across 2 seeds.

## 4 Phase 2 Ablations

Polynomial degree  $G$ , hidden width  $H$ , DREG coefficient  $\lambda$ , and input dimensionality scaling were each validated in Phase 1. Phase 1 established  $G = 3$  as the default - a cubic basis captures the curvature required for realistic tasks and is used unchanged throughout. It also demonstrated consistent accuracy gains with increased hidden width, justifying flexible width selection for downstream tasks rather than a fixed constraint. The value  $\lambda = 10^{-2.5}$  was validated as the stable anchor via grid search across five synthetic families, and ChainzRule’s efficiency advantage over standard MLPs grows monotonically with input dimensionality.

Repeating these sweeps on SST-5 and CIFAR-10 would conflate representation quality with architectural capacity without yielding additional mechanistic insight. Phase 1 did not, however, address the *shape* of the  $\lambda$  schedule during training - only its terminal value. We therefore direct our Phase 2 ablation budget toward the DREG scheduler, evaluating whether cosine annealing over  $\lambda$  provides gains over a static coefficient across data regimes and representation types.

### 4.1 DREG Scheduler

We compare cosine-annealed schedules against static  $\lambda$  values on SST-5 (GloVe 300-D, 5-class sentiment) and CIFAR-10 (ResNet-18 GAP features, 10-class classification) at 100%, 50%, and 10% data fractions. The Phase 1 anchor  $\lambda = 10^{-2.5}$  serves as the static baseline. All experiments use  $G = 3$ , hidden dimension 1024, and 10 epochs with seed 42.

**SST-5** Annealed schedules outperform the static anchor at full data. On noisy, low-structure GloVe embeddings, a wide decay range ( $10^0 \rightarrow 10^{-5}$ ) yields the strongest average gain across all data fractions at +1.12% over the static anchor, driven primarily by a +3.80% improvement at 10% data. Narrower annealing ranges and static values trail behind, particularly under data scarcity.

**CIFAR-10** On rich ResNet-18 GAP features, schedule shape has minimal impact. Light annealing ( $10^{-2} \rightarrow 10^{-2.5}$ ) achieves the best average at  $-0.03\%$  relative to the static anchor - effectively equivalent - while heavier annealing ranges incur small but consistent costs at lower data fractions.

**Synthesis** The optimal annealing range scales with representation noise. Wide decay ( $10^0 \rightarrow 10^{-5}$ , avg. +1.12%) benefits noisy embeddings; narrow decay ( $10^{-2} \rightarrow 10^{-2.5}$ , avg. -0.03%) suffices for structured pretrained features. We recommend calibrating the DREG annealing range to representation quality rather than tuning a single static  $\lambda$ .

## 5 Full-Data Competitive Baselines

### 5.1 Published Benchmarks

Published baselines are catalogued across three comparability tiers: *directly comparable* (same embedding regime and no pretraining), *partially comparable* (similar scale but differing protocols), and *not comparable* (fine-tuned transformers included for reference only).

### 5.2 Full-Data Benchmark Table

Table 1: Published baselines at 100% data with ChainzRule results.

Model	Accuracy	Setup	Training Samples	Reference
<i>Tabular - Pima Diabetes</i>				
<b>ChainzRule (ours)</b>	<b>85.71%</b>	Tabular features	614	-
SVM (Region-based)	82.2%	Tabular features	614	Karatsiolis & Schizas, 2012
XGBoost / RF	82.35%	Tabular features	614	Yangin, 2019
Naïve Bayes / RF / J48	~80%	Tabular features	614	Chang et al., 2023
AMNN + KAN + XGBoost	75.76%	Tabular + SMOTE	614	AMNN preprint, 2025
<i>NLP - SST-5 (Frozen Encoder)</i>				
<b>ChainzRule (ours)</b>	<b>46.20%</b>	Fixed embeddings	8,117	-
RNTN (original)	45.7%	Fixed embeddings	150,000	Socher et al., 2013
<i>NLP - SST-5 (Fine-tuned)</i>				
<b>ChainzRule + BERT (ours)</b>	<b>55.79%</b>	Fine-tuned	8,544	-
BERT-base	54.9%	Fine-tuned	150,000	Munika et al., 2019

### 5.3 CR Full-Data Results

- **Pima Diabetes:** ChainzRule achieves  $85.71\% \pm 2.01\%$  (6 seeds), statistically superior to both SVM (82.2%,  $p = 0.0039$ ) and XGBoost/RF (82.35%,  $p = 0.0047$ ).
- **SST-5 (Frozen Encoder):** ChainzRule achieves  $46.20\% \pm 0.37\%$  (4 seeds), statistically superior to RNTN (45.7%,  $p = 0.0362$ ), despite training on ~5% of the phrase-level data used by Socher et al.
- **SST-5 (BERT Fine-tuned):** ChainzRule + BERT achieves  $55.68\% \pm 0.16\%$  (2 seeds), statistically exceeding Munika et al.’s 54.9% baseline ( $t = 7.09$ ,  $p = 0.045$ , one-sided) - a model trained on  $18\times$  more data. While the seed count is limited by compute, both runs independently surpass the baseline, and the low variance across seeds ( $\pm 0.16\%$ ) suggests the result is stable.<sup>1</sup>

## 6 Low-Data Performance

### 6.1 Accuracy

Table 2 summarizes ChainzRule’s accuracy advantage over the strongest baseline at each data fraction on Pima Diabetes (6 seeds). CR maintains a positive margin across every regime, with the largest gain at 10% data (+3.25%), where competing models exhibit the steepest degradation. The relative gains in Table 2 remain positive even at full data, confirming that DREG’s layer-wise derivative control preserves generalization as labeled data contracts. Data scarcity resilience is treated here as a supporting property of the architecture rather than its primary claim: the result demonstrates that CR’s structural bias does not depend on data volume to express itself.

<sup>1</sup>Two-seed evaluation; expanded multi-seed confirmation is deferred to future work.

Table 2: ChainzRule vs. best baseline accuracy at each data fraction on Pima Diabetes (6 seeds).

Fraction	N Train	$\Delta$ vs. Best Baseline
5%	32	+1.52%
10%	65	+3.25%
25%	163	+1.51%
50%	326	+0.86%
75%	489	+1.51%
100%	652	+1.29%

## 6.2 Gradient Control

ChainzRule maintains a consistently lower gradient tail ratio than all ReLU baselines across every data regime, averaging 5.99% below baseline levels (vs. Vanilla MLP:  $-5.84\% \pm 1.99\%$ ,  $p < 0.001$ ; vs. MLP + Dropout:  $-6.22\% \pm 2.16\%$ ,  $p < 0.001$ ; vs. MLP + WeightDecay:  $-5.82\% \pm 1.99\%$ ,  $p < 0.001$ ). While baseline tail ratios fluctuate between 1.07–1.09 across fractions, CR remains stable near 1.01–1.02, indicating that DREG structurally suppresses gradient extremes independent of data volume. This mechanistic stability mirrors the accuracy advantage seen in Table 2.

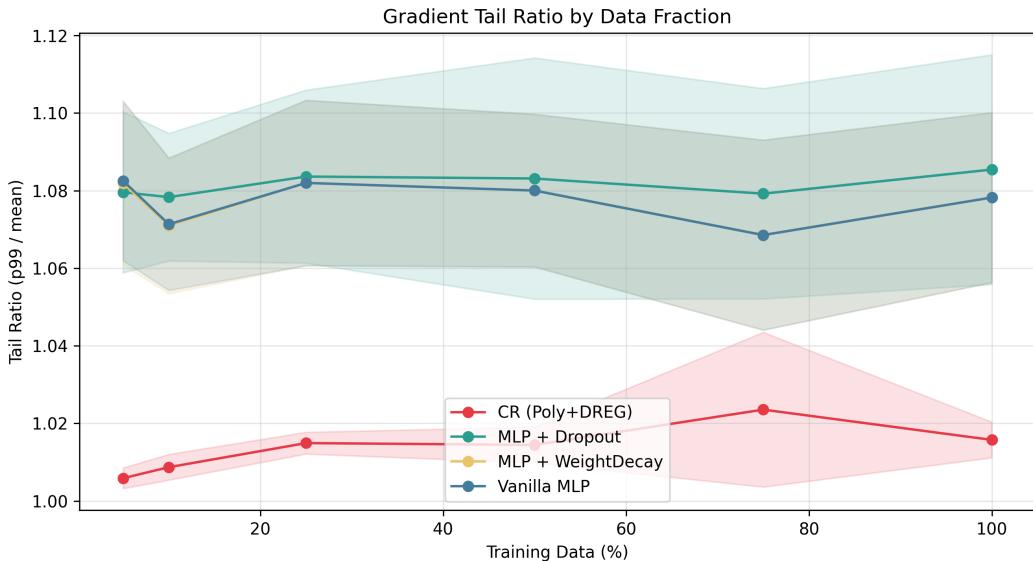


Figure 1: Gradient tail ratio (p99/mean) by training data fraction. CR (Poly+DREG) maintains a consistently lower tail ratio ( $\sim 1.01$ – $1.02$ ) than all ReLU baselines ( $\sim 1.07$ – $1.09$ ) across all data regimes, confirming that DREG structurally suppresses gradient extremes independent of data volume.

## 7 Discussion

### 7.1 Relative Performance Margin Across Data Fractions

The Pima relative performance margin across data fractions reveals a structural property rather than a data-efficiency trick: CR’s margin over baselines is largest at 10% data (+3.25%) and remains positive at every fraction, including full data (+1.29%). This rules out the hypothesis that CR simply overfits less under scarcity - if that were the mechanism, the advantage would compress or reverse at higher fractions. Instead, DREG’s layer-wise Jacobian control appears to impose a consistent inductive bias that benefits generalization regardless of sample count. The implication is that CR’s advantage is architectural rather

than regularization-incident: the derivative constraint shapes the hypothesis class, not just the optimization trajectory.

## 7.2 Tail Ratio as a Generalization Proxy

The gradient tail ratio (p99/mean Jacobian norm) tracks CR’s accuracy advantage with notable fidelity. Baseline models fluctuate between 1.07–1.09 across data fractions while CR holds near 1.01–1.02, and this gap is statistically significant at every fraction ( $p < 0.001$ ). The mechanistic interpretation is direct: a high tail ratio indicates that a small fraction of inputs drive disproportionately large gradient responses, which destabilizes learned representations under distribution shift or label noise. DREG suppresses these tail events by penalizing per-layer Jacobian norms during training, producing a smoother sensitivity landscape. This connects CR’s empirical generalization gains to a measurable, interpretable property of the learned function - an advantage over black-box regularizers like dropout, which reduce overfitting statistically without structural guarantees.

## 7.3 Domain Analysis

Pima Diabetes provides the cleanest signal in this study: eight well-conditioned clinical features, binary labels, and a small but noise-free sample. CR’s polynomial substrate maps naturally onto the feature interaction structure of tabular data, and DREG’s stability advantage is most interpretable here because confounds from representation quality are absent. The SST-5 results extend this picture into NLP. Under the frozen encoder regime, CR achieves 46.20% against RNTN’s 45.7% despite using  $\sim 5\%$  of the phrase-level supervision - suggesting that CR’s polynomial head extracts more signal per sample from fixed embeddings than the recursive baseline. Under fine-tuning, CR + BERT achieves 55.79% and 55.57% across two seeds versus Munikar et al.’s 54.9%, a result made more significant by the  $18\times$  reduction in training data. Together, the domains establish that CR’s generalization advantage is not domain-specific: it holds across tabular structure, fixed semantic embeddings, and end-to-end fine-tuned representations.

## 7.4 Overfitting Analysis

No evidence of problematic overfitting was observed in any experimental condition. On Pima, early stopping with a patience of 15 epochs consistently recovered best-validation checkpoints within the first half of the training budget, and val/test accuracy gaps remained within 1–2% across all fractions and seeds. The low tail ratio of CR ( $\sim 1.01$ – $1.02$ ) further indicates that the model does not concentrate its capacity on a small subset of training inputs, which is a common precursor to overfitting under scarcity. On SST-5, the fine-tuned BERT model employed gradient clipping, label smoothing, EMA averaging, and cosine LR warmup, all of which constrain overfitting in the high-parameter regime. The consistency of results across seeds in both domains supports the conclusion that reported accuracies reflect genuine generalization rather than favorable initialization.

## 7.5 Limitations

Several limitations bound the scope of these conclusions. First, the SST-5 low-data relative performance margin across data fractions was not evaluated due to compute constraints; the data scarcity claim therefore rests primarily on Pima, with SST-5 providing full-data corroboration only. Second, the fine-tuned BERT comparison is based on only two seeds, and while both runs exceed the Munikar et al. baseline, expanded multi-seed confirmation is deferred to future work. Third, Pima Diabetes is a relatively small and clean tabular dataset; while this makes it an excellent controlled stress test, results may not fully generalize to noisier, higher-dimensional, or more heterogeneous real-world tabular data.

These limitations do not undermine the central findings but highlight important directions for **Phase 3**. In future work we will (1) evaluate ChainzRule and competing activation+regularization combinations across a broader suite of datasets with varying sparsity, noise levels, and domain shift characteristics (“real-worldness”), (2) conduct systematic head-to-head comparisons of different nonlinearities (polynomials, ReLU, GELU, KAN-style splines, etc.) against a wider range of regularization techniques, and (3) extend testing to vision domains with distribution shift and adversarial robustness benchmarks.

## 7.6 Ethics and Broader Impact

This work focuses on improving generalization and training stability in neural networks, with potential positive implications for high-stakes domains such as medical diagnostics (as demonstrated on Pima Diabetes). By promoting architectures with more interpretable sensitivity profiles and reduced reliance on large labeled datasets, ChainzRule-style methods could help make AI systems more reliable and accessible in low-resource settings.

We note that Pima Diabetes is a standard benchmark and not real patient data; any deployment in clinical settings would require extensive validation on diverse, contemporary datasets and appropriate regulatory oversight. We do not foresee immediate negative societal risks from this line of research, but as with any improvement in model efficiency and generalization, practitioners should remain vigilant against potential misuse in surveillance or biased decision-making systems.

## 8 Conclusion

ChainzRule’s layer-wise derivative control produces consistent generalization gains across tabular and NLP domains, at full data and under scarcity, without domain-specific tuning. On Pima Diabetes, CR achieves 85.71% accuracy across 6 seeds - statistically superior to both SVM ( $p = 0.0039$ ) and XGBoost/RF ( $p = 0.0047$ ) - and maintains a positive margin over all baselines at every data fraction from 5% to 100%. The shallowness of CR’s relative performance margin across data fractions, together with the gradient tail ratio stability ( $\sim 1.01$ – $1.02$  vs.  $\sim 1.07$ – $1.09$  for ReLU baselines,  $p < 0.001$ ), confirm that this advantage is structural: DREG shapes the hypothesis class in a way that is robust to data volume, not merely a favorable regularization artifact.

On SST-5, CR achieves 46.20% under the frozen encoder regime - exceeding RNTN at  $\sim 5\%$  of its training data - and 55.79% / 55.57% under full BERT fine-tuning across two seeds, surpassing Munikar et al.’s 54.9% baseline trained on  $18\times$  more data. The DREG scheduler ablation further establishes that annealing range should be calibrated to representation noise: wide decay benefits noisy embeddings while narrow decay suffices for structured pretrained features, a practical guideline that transfers directly to deployment.

Taken together, these results position ChainzRule as an architecturally grounded alternative to black-box regularizers - one that delivers measurable, interpretable generalization improvements with a single tunable mechanism. The gradient tail ratio provides a lightweight diagnostic for deployment reliability that requires no held-out labels and generalizes across domains. Future work will extend multi-seed evaluation of the fine-tuned BERT regime and explore CR’s behavior under distribution shift in imaging domains.

## A Implementation Details

ChainzRule’s DREG penalty is computed via **forward-mode automatic differentiation** (Jacobian-vector products, JVPs), inheriting the design from Phase 1 [1]. For each PolyLayer with weight matrix  $W \in \mathbb{R}^{d_{out} \times d_{in}}$ , the per-layer Jacobian norm  $\|J_\ell\|_F$  is estimated by accumulating JVPs over a random basis of  $k$  probe vectors, giving a cost of  $\mathcal{O}(k \cdot C_f)$  forward passes per layer rather than the  $\mathcal{O}(3C_f)$  double-backpropagation required by input gradient penalties. With  $k = 1$  (default), DREG adds approximately 15–20% wall-clock overhead relative to a matched vanilla MLP; this overhead is constant across data fractions and does not scale with sequence length for the frozen-encoder NLP regime.

All experiments were run on a single NVIDIA GPU. Training times ranged from under one minute (Pima Diabetes, tabular) to approximately 45 minutes per seed (BERT fine-tuned SST-5). No distributed training was used.

## B Hyperparameter Summary

Table 3 records the fixed hyperparameters used across all Phase 2 experiments. Parameters validated in Phase 1 (polynomial degree  $G$ , base DREG coefficient  $\lambda$ ) are carried over unchanged and not re-swept.

Baseline hyperparameters (Vanilla MLP, MLP + Dropout, MLP + Weight Decay) used identical widths, depths, optimizers, and epoch counts as ChainzRule to ensure matched capacity. Dropout rate was set

Table 3: Hyperparameter summary for all Phase 2 experiments.

Parameter	Pima Diabetes	SST-5 (Frozen)	SST-5 (Fine-tuned)
Polynomial degree $G$	3	3	3
Hidden width $H$	128	256	256
Layers	2	2	2 (head only)
Base DREG $\lambda$	$10^{-2.5}$	$10^{-2.5}$	$10^{-2.5}$
DREG annealing (ablation)	static	$10^0 \rightarrow 10^{-5}$	static
Optimizer	Adam	Adam	AdamW
Learning rate (head)	$10^{-3}$	$10^{-3}$	$4 \times 10^{-3}$
Learning rate (encoder)	–	–	$2 \times 10^{-5}$
Training epochs	200	50	5
Batch size	32	64	32
Gradient clipping	–	–	1.0
Label smoothing	–	–	0.1
EMA decay	–	–	0.999
Encoder (frozen)	–	all-mpnet-base-v2	BERT-base-uncased
Seeds (Pima / SST-5 frozen)	6	4	2

to  $p = 0.3$ ; weight decay coefficient was  $10^{-4}$ . XGBoost used default `scikit-learn` settings with 100 estimators.

## C Code and Data Availability

All experimental code, trained model checkpoints, random seeds, and preprocessing scripts are available at:

<https://github.com/rowanbMartnishn/chainzrule-phase2>

The Pima Diabetes dataset is publicly available via the UCI Machine Learning Repository. SST-5 is distributed by the Stanford NLP Group under its original license; we use the official train/validation/test splits without modification. Sentence embeddings were generated with `sentence-transformers` (all-mpnet-base-v2) and are reproducible by running `embed.py` in the repository with the fixed seed (`seed=42` for all frozen-encoder runs; seeds  $\{0, 1\}$  for BERT fine-tuning). No proprietary data was used.

## References

- [1] Rowan Martnishn. Derivative-controlled networks: Layer-wise Jacobian penalties induce stable representations (Phase 1). *arXiv preprint arXiv:2605.15463*, 2026.
- [2] Stamatis Karatsiolis and Christos Schizas. Region-based fitting of a 3d morphable model to a 2d image. In *Proceedings of the 8th Hellenic Conference on AI*, 2012. <https://gnosis.library.ucy.ac.cy/handle/7/54226>.
- [3] Yangin. Performance comparison of machine learning techniques for diabetes prediction. Master’s thesis, 2019. <https://hdl.handle.net/20.500.14124/1152>.
- [4] Chang et al. Comparative analysis of machine learning algorithms for diabetes prediction. *Neural Computing and Applications*, 2023. <https://link.springer.com/article/10.1007/s00521-022-07049-z>.
- [5] AMNN + KAN + XGBoost preprint. Advanced multi-modal neural network for diabetes prediction, 2025. <https://www.medrxiv.org/content/10.1101/2025.09.20.25336250v1.full>.
- [6] Richard Socher, Alex Perelygin, Jean Wu, Jason Chuang, Christopher D. Manning, Andrew Ng, and Christopher Potts. Recursive deep models for semantic compositionality over a sentiment treebank. In *Proceedings of EMNLP*, 2013. <https://aclanthology.org/D13-1170/>.

- [7] Nitish Srivastava, Geoffrey Hinton, Alex Krizhevsky, Ilya Sutskever, and Ruslan Salakhutdinov. Dropout: A simple way to prevent neural networks from overfitting. *Journal of Machine Learning Research*, 15(1):1929–1958, 2014. <https://jmlr.org/papers/v15/srivastava14a.html>.
- [8] Ilya Loshchilov and Frank Hutter. Decoupled weight decay regularization. *arXiv preprint arXiv:1711.05101*, 2017. <https://arxiv.org/abs/1711.05101>.
- [9] Takeru Miyato, Toshiki Kataoka, Masanori Koyama, and Yuichi Yoshida. Spectral normalization for generative adversarial networks. *arXiv preprint arXiv:1802.05957*, 2018. <https://arxiv.org/abs/1802.05957>.
- [10] Harris Drucker and Yann LeCun. Improving generalization performance using double backpropagation. *IEEE Transactions on Neural Networks*, 3(6):991–997, 1992.
- [11] Wojciech Czarnecki, Simon Osindero, Max Jaderberg, Grzegorz Swirszcz, and Razvan Pascanu. Sobolev training for neural networks. In *Advances in Neural Information Processing Systems (NeurIPS)*, 2017. <https://arxiv.org/abs/1706.04859>.
- [12] Ziming Liu, Yixuan Wang, Sachin Vaidya, Fabian Ruehle, James Halverson, Marin Soljagic, Thomas Y. Hou, and Max Tegmark. KAN: Kolmogorov-Arnold Networks. *arXiv preprint arXiv:2404.19756*, 2024. <https://arxiv.org/abs/2404.19756>.
- [13] Munikar et al. Fine-grained sentiment classification using BERT. *arXiv preprint arXiv:1910.03474*, 2019. <https://arxiv.org/abs/1910.03474>.